Instabilities of a persistent-photoconductivity semiconductor associated with heat transfer to a He-II film

M. Dong, D. Baum,* and A. Honig
Physics Department, Syracuse University, Syracuse, New York 13244
(Received 13 May 1996)

An instability characterized by an *S*-shaped *I-V* characteristic of the persistent photoconductivity (PPC) of CdS crystals is explained by the heat transport across the interface of the crystal surface and a He-II film. The model is based on the complete evaporation of the He-II film, which occurs at a heat flux lower than the conventional peak flux in bulk liquid He-II, and furthers our understanding of supercriticality and the anomalous power dependence of the Kapitza resistance at the interface of solids and liquid He-II. The PPC, characteristic of compensated CdS at low temperatures, provides *light-dose*-dependent variable conductivity, a very useful degree of freedom for the heat-transfer investigations. [S0163-1829(96)03744-7]

I. INTRODUCTION

Persistent photoconductivity (PPC) in CdS semiconductors has been extensively studied. Nevertheless, some fundamental aspects are still not totally resolved. In the course of a broad program aimed at understanding the fundamental origin of the PPC in CdS using low-temperature luminescence[1] and transport[2] measurements, discontinuities in the persistent conductivity at temperatures below the liquid-helium λ point were observed.[3,4] Until the recent work[5] to be reported in detail here, these were attributed to an electronic mechanism which provided a plausible account of some, but not all, of the behavior.[6] We now believe that all of the observed phenomena can be accounted for with a thermal model of the interface of a superfluid helium film with the semiconductor. Phenomenologically similar discontinuities in other systems have been reported, with several different mechanisms proffered as explanations. These will be briefly reviewed below. In this paper we present and analyze electronic phenomena and relate these to different inferred characteristics of liquid-helium superfluid films.

Discontinuities associated with a negative differential conductivity have been reported for various types of semiconductors and other systems.[7] There are two types of current-voltage (*I-V*) curves exhibiting discontinuities. One is defined as *S* shaped where the discontinuity occurs in the current when the voltage varies. The other is defined as *N* shaped in which the discontinuity occurs in voltage as the current varies. The details of the physical origin for the phenomena vary from system to system, but generally they can be divided into two categories: (i) A switch in of a different conduction mechanism,[7] used to explain the *N*-shaped *I-V* curves in two-valley semiconductors and the *S*-shaped curves in shallow-impurity compensated Ge and Si. (ii) Superheating mechanisms, in which electric-field-induced self-heating produces the discontinuities through the temperature dependence of the conductivity. Specifically, for a conductivity $\sigma(T)$, we have the heat-balance equation:

$$\sigma[\Delta T(E)+T_0]E^2=P_C[\Delta T(E)+T_0], \tag{1}$$

where $\sigma[T(E)]$, E, and $P_C[T(E)]$ are the electrical conductivity, electric field, and cooling power per unit volume, respectively. T_0 is the ambient temperature and ΔT, which is determined by E, is the temperature difference between either the electron reservoir and the lattice (when the lattice is in thermal equilibrium with ambient) or the lattice and ambient (when the electrons are in thermal equilibrium with the lattice). Thus the effect of E-field-induced self-heating on the $\sigma[T(E)]$ determines the *I-V* characteristic. For certain $\sigma(T)$ functions, the solution of the heat-balance equation has a singularity $\sigma_d=dj/dE=\infty$, where j is the current density, which marks the point where the discontinuity occurs in *S*-shaped *I-V* curves. Instabilities in *I-V* curves for many systems[7–9] have been interpreted as due to this mechanism. In principle, another type of singularity, $\sigma_d^{-1}=dE/dj=\infty$, could occur, which would mark the point of instability in *N*-shaped curves. In both situations, the instabilities are associated with a specific form of $\sigma[T(E)]$. In this paper, we propose a first instance, to our knowledge, where a discontinuity in the cooling power $P_C(T)$ also can result in an *S*-shaped *I-V* curve. The observed *S*-shaped *I-V* curve is for the PPC of CdS and the cooling mechanism in question is the heat transfer from the solid to the adsorbed superfluid helium film which provides evaporative cooling until the film completely evaporates away as a consequence of the inability of the recondensation rate to keep up with the evaporation rate of the helium film.

Two relevant issues in the problem of heat transport across a boundary are the power dependence of the Kapitza resistance[10] and the peak heat flux.[11] It is known that a heat flux flowing across a boundary between liquid helium and a solid results in a temperature discontinuity. The related thermal boundary resistance, known as the Kapitza resistance[12] R_K, is defined as the ratio of the temperature discontinuity, ΔT, to the heat flux Q:

$$R_K=\Delta T/Q. \tag{2}$$

Although agreement between the theoretical and experimental values of R_K is still largely qualitative in some systems, it is generally accepted that a heat flux carried by phonons across a boundary can be described by

$$Q=\sigma_{K_P}(T_s^4-T_{\mathrm{He}}^4), \tag{3}$$

where T_S and T_{He} are the temperatures of the solid and of liquid helium, respectively, and σ_{K_P} is the coefficient which is analogous to the Stephan-Boltzmann constant in black body radiation. Based on Eqs (2) and (3), it can be seen that for small enough Q, R_K is independent of Q, implying a linear relationship in ΔT vs Q. However, when Q is large, R_K decreases as Q increases. It is found experimentally that there exists an opposite type of nonlinearity in this problem, where the Kapitza resistance increases rather than decreases with increasing Q. Because this is contrary to Eqs. (2) and (3), it is referred to as the anomalous power dependence of the Kapitza resistance. The first experiments exhibiting this effect were with Cu-He-II and Pt-He-II interfaces.[10] Since that first publication, there have been other reports confirming the discovery and purporting to explain the anomalous power dependence of the Kapitza resistance in terms of a combination of surface impurities and supercriticality,[13] a situation where dissipation arises in the superfluid helium.

It should be noted here that in the literature, there is another phenomenon referred to as ''anomalous Kapitza resistance,'' distinct from the anomalous *power dependence of* the Kapitza resistance we have been discussing. In the anomalous Kapitza resistance, the anomaly is in the form of the increase in Kapitza resistance when the temperature approaches the λ point of liquid helium, which is contrary to the T^3 dependence of Eqs. (2) and (3). This anomalous Kapitza resistance was first mentioned by White, Gonzales, and Johnson,[14] and later was systematically investigated by several groups.[15–17] The anomaly is understood now as due to the divergence of the singular component in the Kapitza resistance as the λ point is approached. Our effects occur at temperatures significantly below the λ point, and hence this mechanism doesn't manifest itself in this present report.

The peak heat flux represents a heat influx limit above which the thermal conductivity of superfluid He-II, generally considered infinite (implying an unlimited capacity to carry away heat), becomes finite due to formation of a gas film and consequent quenching of superfluidity.[11] This peak heat flux in bulk liquid helium has been measured to be in the range of 1–10 W/cm^2. A process involving the evaporation of the superfluid helium film, having a similar effect to peak heat flux, is discussed in this paper. In our experiments, the peak flux which gives rise to the gas film is not reached, because the superfluid helium film in the regime of our discontinuities evaporates at considerably lower heat fluxes. That evaporation results in the separation of the sample from the liquid helium by the helium gas, resulting is a situation similar to that occurring in the more usual bulk-helium peak flux case.

II. EXPERIMENT

The samples used in this study were cut from compensated n-type single-crystal CdS, designated Eagle-Picher grade EP-A, with room-temperature resistivities of about 10^{10} Ω-cm. Once cut to a convenient size, typically 5×1×1 mm, the surfaces of the samples were mechanically polished with 400 grit Si:C abrasive powder to remove gross blemishes. A mirror finish was then obtained by successive polishings with 1.0 and 0.3-μm α-alumina and 0.05-μm γ-alumina powder, followed by etching in a hydrochloric acid solution of the volume ratio two parts concentrated HCl to one part water. Indium contact pads were deposited and electrical leads were attached to the pads with a bakeable silver paste. The absence of non-Ohmic effects was established using a standard four-point probe.

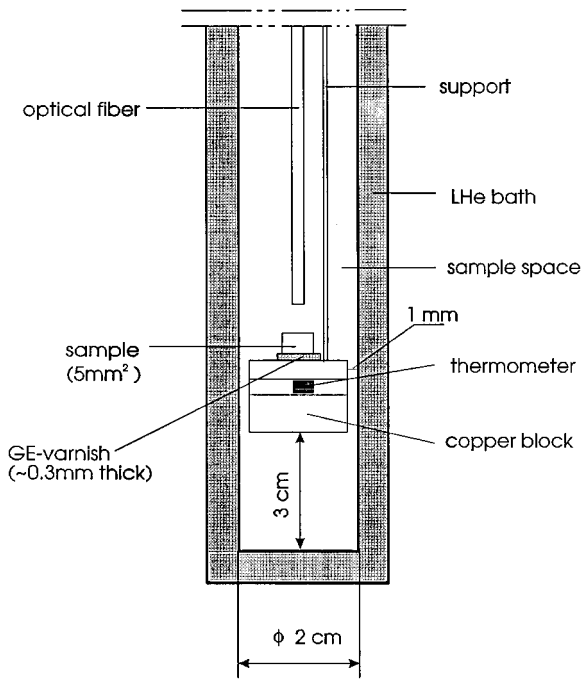

FIG. 1. Schematic diagram of the sample cell. The sample is high resistivity CdS. Variable amounts of exchange gas (condensable at low enough liquid-helium bath temperatures) are employed.

The experimental setup, a simple configuration suitable for photoconductivity and photoluminescence experiments,[1,2] is shown in Fig. 1. The sample is mounted on a copper block suspended in the sample space, kept in thermal contact by means of helium exchange gas in the sample space. Light is transmitted to the sample through a fiber-optic light guide. The liquid reservoir could be kept at any temperature between 1.2 and 4.2 K. By controlling the amount of helium gas in the sample space, three different conditions could be established: (1) The gas-film condition, where the pressure is less than the vapor pressure corresponding to the helium bath temperature. For the surface at the bottom of a cell, the gas film thickness, d, depends on pressure, p, through the equation[18]

$$-k_BT\ \ln(p/p_{\mathrm{SVP}})=\alpha/d^3, \tag{4}$$

where α is a constant characterizing the van der Waals interaction between the helium and the solid surface. When p approaches the saturation vapor pressure value, p_{SVP}, d approaches infinity. In some of the literature, what we call gas film and liquid film (see next condition) are referred to as film and bulk, respectively. (2) The liquid-film condition, where the initial amount of helium introduced into the sample space results in some liquefaction at the bottom of sample space, but not enough for the sample to touch the liquid pool; and (3) The bulk condition, where the sample is

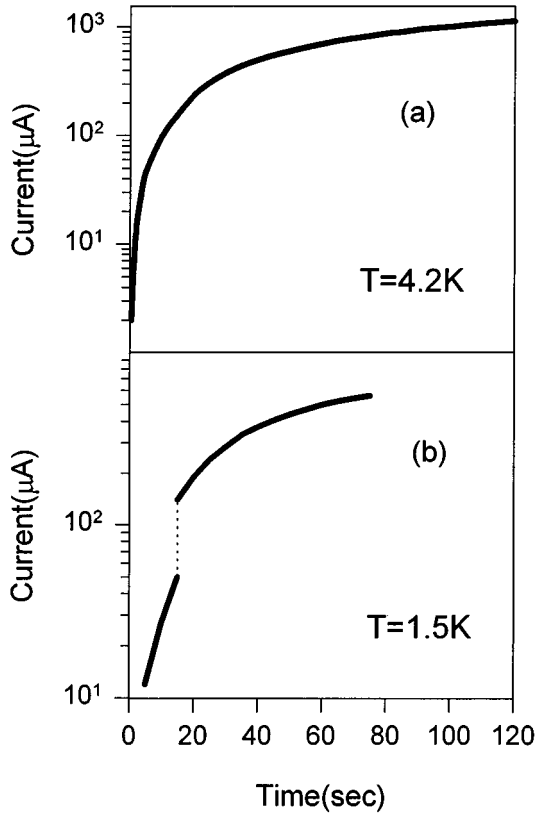

FIG. 2. PPC buildup at (a) 4.2 K; (b) 1.5 K. The voltage is 5 V, and liquid-film condition (2) applies.

completely immersed in bulk liquid helium. It should be noted that the experimental design was for general photoconductivity measurements, and was not optimized for the study of the effects reported here. Nevertheless, the geometry turns out quite suitable for the effects addressed in this report.

III. CHARACTERISTICS OF THE INSTABILITIES

The samples exhibit persistent photoconductivity (PPC). The mechanism for PPC in this type of sample is not yet unequivocally established, but it is widely believed that in highly compensated CdS compound semiconductors, potential barriers caused by the randomly distributed charge centers are responsible[19] for the PPC. All the I-V curves shown in this section were obtained in a voltage-controlled mode. Figure 2 shows two PPC buildup processes at $T=4.2$ and $T=1.5$ K, with illumination commencing at time $t=0$. Referring to Fig. 2(a), the photocurrent rises continuously with irradiation time. If the light is switched off at any moment, the photocurrent decays very slowly. Generally after about an hour, the photoconductivity remains almost constant, at an appreciable fraction (usually 80% for the light intensities that we use) of its value at the moment of cessation of the illumination. This growth of PPC saturates, with the time to reach saturation inversely proportional to the light intensity. This means the conductivity can be controlled by a light dose (integrated light intensity) over a wide range (at least five orders of magnitude). We specify the PPC level, a measure of the integrated light intensity, by the fraction of the saturation current after relaxation ceases. As will be seen, this

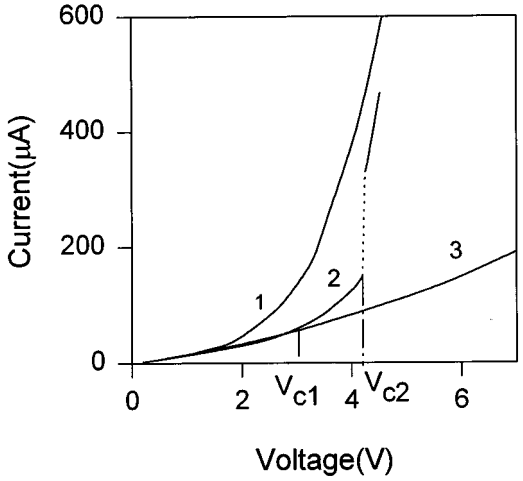

FIG. 3. PPC I-V characteristics at various helium conditions: curve 1, gas-film condition; curve 2, liquid-film condition; curve 3, liquid-bulk condition. $T=1.5$ K.

control with light dose of the sample's conductivity is a very useful feature for this study.

The essential elements of the phenomena that we report here are illustrated in Fig. 2. In this plot of the PPC current, I, vs light-irradiation time, taken at $V=5$ V, the PPC current grows with light-irradiation time, until an unstable point is reached, signified by a jump in current. This is evident in Fig. 2(b) near $t=15$ sec, corresponding to a PPC level of approximately 10%. The effect is seen only when $T<2.18$ K, the λ point of liquid helium [contrast with Fig. 2(a)]. In Fig. 3, the effect of the helium environment on this instability is shown. The instability is only observed when the helium temperature is below the liquid-helium λ point (2.18 K), and only for the *liquid-film condition* denoted as condition (2) above. As shown in the figure, at very low voltages (below 1.5 V) the I-V curves in the three conditions are nearly identical. Above 1.5 V, the curve in condition (1) rises rapidly

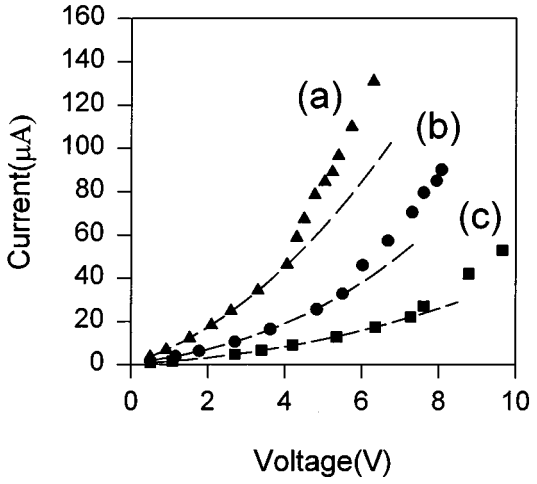

FIG. 4. PPC I-V characteristics for three light doses: (a) near saturation PPC current; (b) $\frac{1}{3}$ saturation; (c) $\frac{1}{6}$ saturation. The last point of each curve is where the jump, characterized later as Q_{C2}, occurs. $T=1.3$ K.

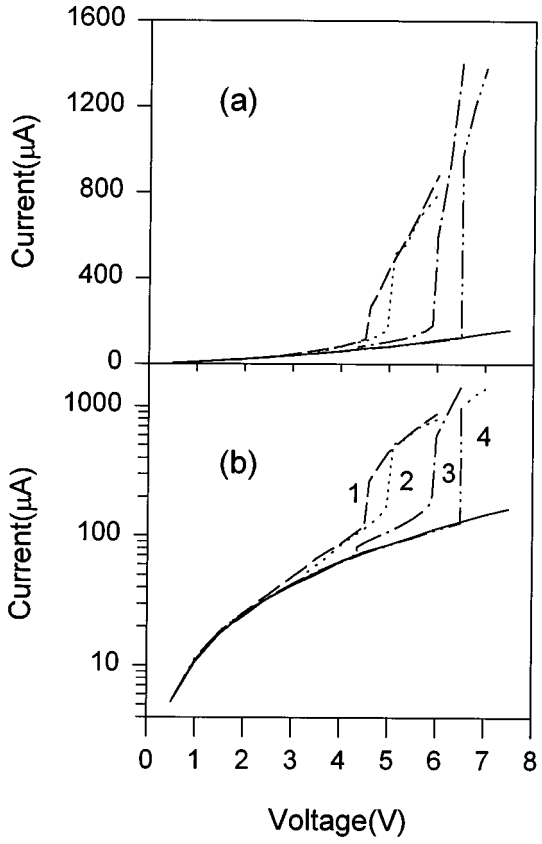

FIG. 5. PPC I-V characteristics under different helium conditions. The solid line is for the liquid-bulk (3) condition. Lines labeled by 1–4 are for I-V curves at the liquid-film (2) condition in the order of increasing amount of helium by equal increments of about 50 cm^3 standard volume of helium gas over the sample space.

but smoothly. The curve in condition (2) breaks away from the one in condition (3) at V_{C1} and becomes unstable at V_{C2}, where it jumps to a new current level that is nearly the same as the one under condition (1). In Fig. 4, the jumps in the current for different PPC levels are shown. The voltages, V_{C1} and V_{C2}, of these curves are very different. However they correspond approximately to the same power levels, which can be taken as evidence of the thermal nature of the instabilities. Furthermore, the experiments show that at the same helium condition, the heating power ($=IV$) at which the instability occurs is the same for the PPC buildup and I-V curves. In view of this constant-power feature, the two critical points denoted by V_{C1} and V_{C2} in Fig. 3 will hereafter also be referred to by Q_{C1} and Q_{C2}. Finally, Fig. 5 shows the variation of the onset voltage of the instabilities with the amount of helium in the pool at the bottom of the sample space. The cause of this dependence is not well understood. It will be discussed in a later section. After curve 4, no change was observed by adding more helium, carried out in successive increments of the same amount as in the previous four.

All of these experimental results provide strong evidence for the thermal nature of the instabilities which leads us to consider the cooling mechanisms. In view of the configuration of the sample cell, there are two cooling routes for the removal of the heat generated in the sample. One is through the helium (in one of the three conditions), and the other is through the GE varnish (GE 7031 by Lakeshore Cryotronics, Inc.) to the copper block. Our model for explaining these features is a variable cooling of the CdS semiconductor via heat transport involving the superfluid He-II film. In the next sections, we analyze the cooling mechanisms, and their role in producing the instabilities. Basically, the effects are due to a sudden loss of cooling, resulting in an immediate temperature rise of the semiconductor. The cooling loss can arise from the anomalous Kapitza thermal resistance, or from the total blow off of the evaporative-cooling He-II film.

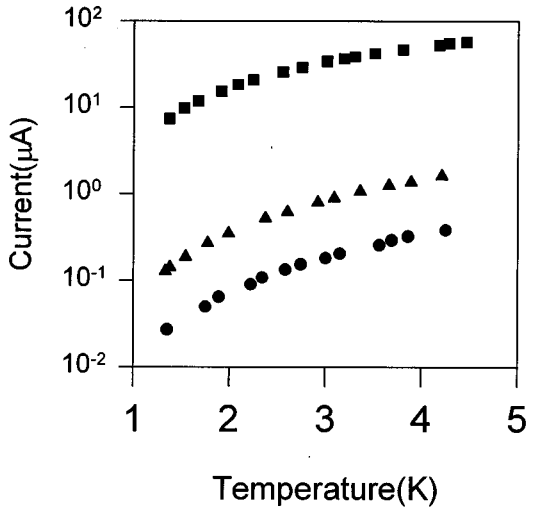

FIG. 6. Temperature dependence of PPC at three light doses: (a) saturation; (b) 3% saturation; (c) 0.7% saturation. $V=0.5$ V.

IV. ANALYSIS

A. Electrical and thermal calibration of PPC

In order to understand the problem quantitatively, a knowledge of PPC current I as a function of light dose D, temperature T, and voltage V is needed. That is, we wish to know the form of the function $I=f(D,T,V)$. For this, measurements of I with various combinations of D,T,V were carried out in the bulk-helium condition. The results are shown in Figs. 6–8. Figure 6 shows the temperature dependence for three doses at $V=0.5$ V. In the relevant region 1.3–2 K, $d(\ln I)/d(\ln T)$, a measure of the PPC current-temperature sensitivity is greater than 1, indicating a stronger than linear temperature dependence of I. Figures 7(a) and 8(a) show the I-V curves, with D and T as parameters. These seemingly different curves can be reduced virtually into one by a reduction procedure as shown in Figs. 7(b) and 8(b). This indicates that the nonlinearity in the I-V curves in the bulk condition is not caused by self-heating, because the ratio of the heating powers is about a factor of 30. Therefore the I-V curves in the liquid-bulk condition give the true characteristics at the ambient temperatures. The results from the reduction procedure also suggest that the voltage dependence of $I=f(D,T,V)$ can be separated from the dose and temperature dependence, i.e.,

$$I=f_1(D,T)f_2(V). \tag{5}$$

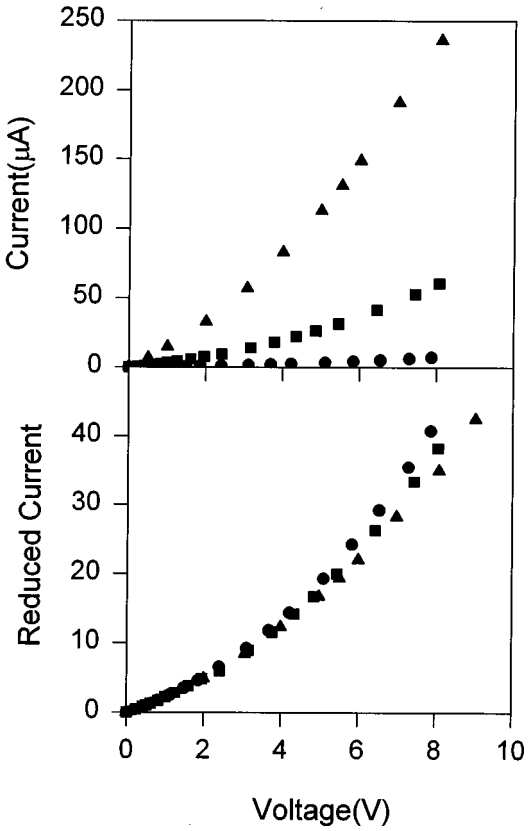

FIG. 7. PPC I-V characteristics for three light doses. From upper to lower curves: 90%, 20%, and 3% of saturation value, respectively. The reduced current figure is obtained by dividing the currents by corresponding values for $V=0.5$ V. This choice of normalization voltage is taken because $V=0.5$ V is used in current vs temperature measurements.

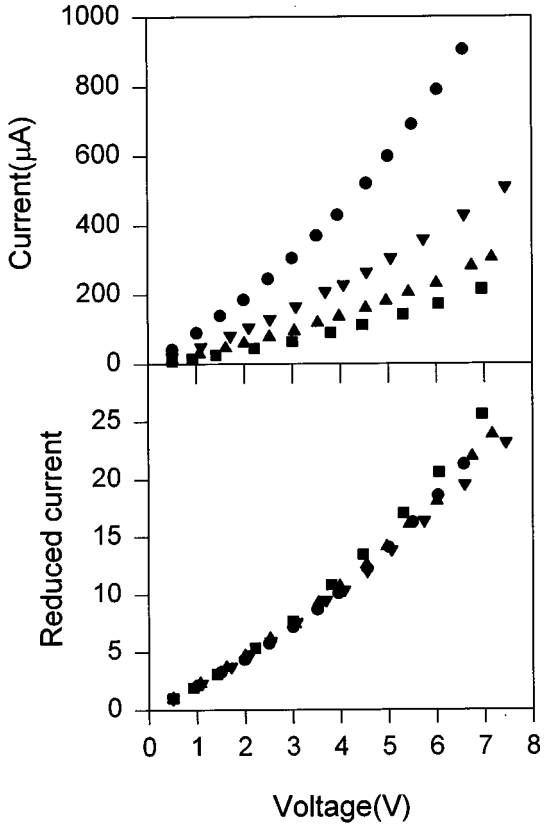

FIG. 8. PPC I-V characteristics at four temperatures. From upper to lower curves, $T=4.2$, 2.7, 2.0, and 1.55 K. Reduced current curves are obtained as described in the caption of the previous figure (Fig. 7).

The form of this expression is similar to the case of conventional photocurrent where I is proportional to $n\mu_e V$. If the mobility μ_e were mainly affected by either D or T, and the carrier concentration n by D, then the separation of the function $I(D, T, V)$ would be straightforward. However, the conduction mechanism here is believed to be hopping, in which case, due to the partial localization of the electronic states, the conductivity depends exponentially on a small power of n and a simple proportionality between I and $n\mu_e V$ is not expected. We will not be concerned at this point with the physics to justify Eq. (5), but will see that it is reasonably in accord with the electrical measurements in the limited domain of interest in our experiments, and will employ it phenomenologically as a means of constructing a quantitative model for the observed effects. Furthermore, we will employ two linear functions for f_1 and f_2, also without any firm theoretical basis:

$$f_1=c_1(D)+c_2(D)T, \tag{6}$$

$$f_2=c_3+c_4V, \tag{7}$$

which conform satisfactorily to the experimental data in the relevant regions.

B. Anomalous power dependence of the Kapitza resistance

We have shown in the previous section (IV A) that I-V curves in the bulk-helium condition exhibit no self-heating. The deviation from those bulk-helium curves of the curves taken in the gas and liquid-film conditions can thus be attributed to the increase of sample temperature due to the self-heating. In the gas-film condition, the current increases rapidly at relatively low voltages, indicating that the cooling power in that condition is small. It has been reported that the effective Kapitza resistance between an adsorbed helium film and a solid depends on the thickness of the film over a limited range of film thickness,[20] or over the entire range.[21] We made a brief attempt to address this issue by examining the self-heating effect at $T=1.3$ K, at various pressures ranging from $p/p_{\rm vap}=10^{-2}$ to slightly below 1, corresponding to a film thickness of from about two layers to essentially infinite layers. No significant difference was observed. Evidently, cooling through gas films is not competitive with cooling via the GE varnish route. This is supported by calculated estimates shown in Sec. IV D.

We will be mainly concerned with the liquid-film condition in the rest of this paper, since that is the case where the thermal breakdown occurs. This corresponds to curve 2 in Fig. 3. In that figure, it is seen that there is no noticeable difference in the I-V curves between liquid-film and bulk conditions when the voltage is smaller than V_{C1}. Above V_{C1}, the current rises faster than it would in the bulk condition, and at V_{C2} it breaks down. In dealing with the problem of

heat transport between solid and He-II, usually one of two approaches is adopted. The approach of treating the problem as an interface one is particularly suitable for the case of heat transfer from solid to bulk He-II, the latter being so efficient in heat transport that it can be considered at ambient temperature except for the case of extremely high heat flux where the superfluidity is quenched. In this case, the thermal impedance is solely determined by the boundary thermal resistance, or Kapitza resistance. The second approach is more applicable to the case where the heat transport is between a solid and a thin isolated layer of helium with several to tens of monolayers.[20] In this condition, the temperature of the film can be considered to be intermediate between that of the sample temperature and the ambient, brought about because the heat transferred from the sample to the (limited heat capacity) liquid-helium film is in series with the heat removed by evaporation of the film into the ambient helium gas atmosphere. In that situation, there is a dynamical balance between evaporation and recondensation of helium gas which is quite complicated, with the gas atmosphere surrounding the film almost certainly not isothermal. Thus, this type of heat transfer is not purely a boundary problem. Nevertheless, it has been treated by the concept of *effective* Kapitza resistance.[20] We will further discuss the heat dissipation mechanism of helium films at the end of this section. We first propose a model to explain the I-V curves in the liquid-film condition.

At low power, the He-II liquid film in our system functions just as bulk He-II to carry away the heat from the solid in the sense that for $Q<Q_{C1}$, the two I-V curves in the liquid-film and bulk conditions are indistinguishable, within our experimental precision. Effectively, the recondensation rate is fast enough to maintain the film. Because of the nonlinearity in the I-V characteristics of the samples, we cannot extrapolate the sample resistance obtained at low-voltage (low power) to the high-voltage region, and thus cannot employ the same technique used in other effective Kapitza resistance measurements.[22] Nevertheless, an upper limit on the difference between the Kapitza resistance in the liquid-film and bulk conditions at low powers can be estimated, based on the precision (about 3%) of our measurements of current. The result turns out to be about 5 K cm^2/W. To our knowledge, there are no data available for the CdS-He-II interface, but this value is comparable to that obtained for the interface[23] of Si and bulk He-II. We attribute the deviation of the I-V curve at Q_{C1} to a mechanism similar to the anomalous power dependence of Kapitza resistance observed in the bulk condition. Specifically, at Q_{C1} the Kapitza resistance rapidly increases, resulting in a temperature increase which is manifested by a slope change in the I-V curves. In Fig. 5, this change of slope takes the form of a smooth fork in curves 1 and 2, and of a jump in curve 3. An explanation for the jump versus the smooth change in slope is that as the power increases, there is positive feedback from the anomalous Kapitza resistance, resulting in a small avalanche effect.

It is interesting to see how the temperature of the sample increases with the heat flux in the region between Q_{C1} and Q_{C2}. Since the difference in the current between the cases of the film and bulk conditions is due to the self-heating, the current in the film condition can be obtained from Eqs. (5) to (7) as

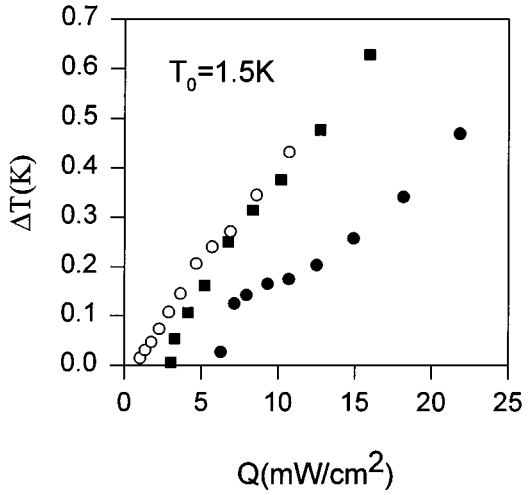

FIG. 9. Temperature increase of sample, ΔT, vs heat flux, Q_h, at successively increasing amounts of helium exchange gas, always within the liquid-film (2) condition. Curves from left to right are for 50 cm^3 successive increments of helium exchange gas. The first and last points on each curve correspond to Q_{C1} and Q_{C2}, respectively. $T=1.5$ K.

$$I_{\text{film}}(V)=f_1(T_0+\Delta T)f_2(V), \tag{8}$$

where T_0 is the ambient temperature and ΔT is the deviation from T_0. All the constants are known from the I-V and I-T curves in the bulk condition as described in the preceding section. Then ΔT can be calculated from Eq. (8) and experimental curve I_{film} vs V:

$$\Delta T=[I_{\text{film}}/f_2(V)-f_1(T_0)]/c_2. \tag{9}$$

In Fig. 9, the relationship between ΔT and Q $(=IV)$ is shown, obtained from the I_{film} vs V curves from Fig. 5 labeled 1–3. The slopes of these curves can be interpreted as an effective Kapitza resistance. Again, this quantity varies with the helium amount. We mention here that the details of the evolution process shown in Figs. 5 and 9 are not perfectly reproducible from run to run, but the trend as displayed is certain. This is not an unusual situation for Kapitza resistance measurements. In addition to the irreproducibility, the dependence on the amount of helium makes the study of precise temperature dependence of these quantities quite complicated, since varying the temperature results in a change in the condensation rate of helium. Despite these difficulties, it still can be seen that the typical onset heat flux of the anomalous power dependence of the Kapitza resistance is of the order of 1 mW/cm^2, which is comparable to or smaller than reported values for the solid and bulk He-II interface.[10,13] Our value of the effective Kapitza resistance is about 150 K cm^2/W, which is significantly larger than for the case of the solid-bulk He-II interface,[10,13] possibly due to recondensation limitations and a warm film, as discussed previously. In the above estimates, the total sample surface area has been used for the flux calculation, without distinguishing the horizontal from the vertical surfaces.

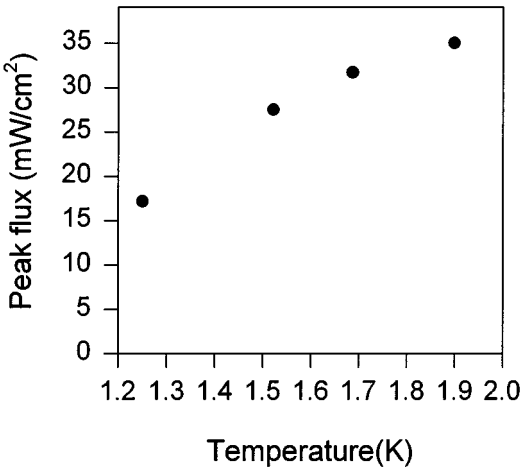

FIG. 10. Peak flux (in the sense of our model of onset of evaporation) vs temperature.

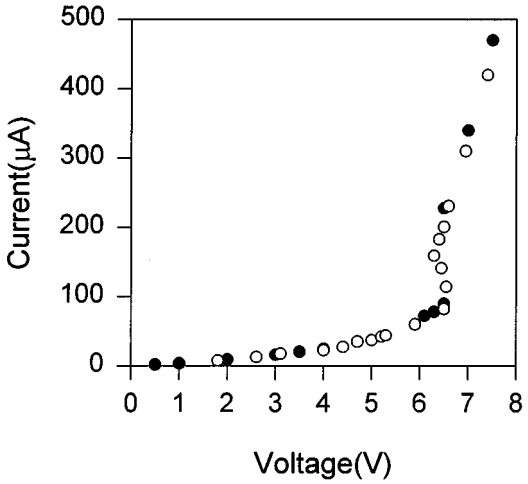

FIG. 11. PPC I-V characteristics under ●—voltage controlled mode; ○—current controlled mode.

C. Film analog of peak heat flux effect

As noted before, a gas film will be formed when a heat flux crossing from a solid to bulk He-II reaches a critical value, known as the peak heat flux. The formation of this gas film certainly causes a dramatic change in the thermal impedance which in turn can result in an instability in the I-V curves. We believe that a process quite similar in its effects, but distinct in its nature, occurs at Q_{C2} in our system. Our conclusion is that a sudden complete helium film evaporation, rather than formation of a gas film, causes a runaway in the temperature of the sample until it reaches a new stable temperature which is determined by a second cooling channel, in this case the heat conduction through the GE varnish to the copper block. This is evidenced by the fact that after the jump in current at Q_{C2}, the resultant current in the liquid-film (2) condition is essentially the same as in the gas-film (1) condition as shown in Fig. 3, indicating the same sample temperature in both cases. As noted earlier, Q_{C2} varies with the amount of helium in the sample space and saturates at a certain point [still in the liquid-film (2) condition]. This saturation value of Q_{C2} as a function of temperature is shown in Fig. 10 which was obtained in one cooling process. There is substantial variability in this type of curve from run to run. Nevertheless, the magnitude of the heat flux corresponding to this saturation Q_{C2} is of the order of 3 mW/cm^2, while the peak heat flux in the solid and bulk He-II interface is in the range[11] of 1–10 W/cm^2. We have attributed this low peak flux mechanism to complete film evaporation, brought about by a limiting rate of helium gas recondensation, in our particular experimental configuration.

To a certain extent both Q_{C1} and Q_{C2} are affected by the amount of helium initially introduced into the sample space, in excess of the amount corresponding to the saturation pressure. The thickness of the condensed liquid helium pool at the bottom of the sample space depends on this quantity, but at the highest amount of gas used, still only corresponds to a liquid-helium pool depth of less than a mm. We do not presently understand this apparent dependence of the thermal conduction circuit on the amount of liquid helium in the pool at the bottom of the sample container. Perhaps the thickness of the liquid film covering the sample, on which the onset heat flux for complete evaporation might be expected to depend, varies with the liquid-helium pool depth. This question seems worthy of further study. A conclusive experiment would require a dedicated design of the sample cell avoiding the open geometry configuration of our present apparatus.

D. S-shaped I-V curves

Controlling voltage and controlling current are two ways to perform measurements of the I-V characteristics. While in the stable region, the two methods are expected to be identical. It is of interest to see what happens in the unstable region. Figure 11 shows a typical I-V curve with points corresponding both to the current-controlled mode and the voltage-controlled mode. It is clear that the former is S shaped, and this is also confirmed by the hysteresis in the voltage-controlled curves (not shown here). This S-shaped I-V curve can be understood by a graphical procedure, which also provides a unified picture of the work discussed in this report.

For the steady state, the heating power equals the cooling power:

$$Q_h(\Delta T) = Q_c(\Delta T), \tag{10}$$

where both sides are regarded as a function of ΔT, the temperature rise of the sample above ambient. The heating power is simply

$$Q_h = IV. \tag{11}$$

The relationship between I and V is given in Eq. (8). For the voltage-controlled case, the heating power is

$$Q_h^V = Vf_2(V)(c_1 + c_2T_0 + c_2\Delta T). \tag{12}$$

For the current controlled case, it becomes

$$Q_h^I = (I/c_4)[I/(c_1 + c_2T_0 + c_2\Delta T) - c_3]. \tag{13}$$

For the cooling powers, there are two channels, as previously described. When the heating power is smaller than Q_{C2}, the

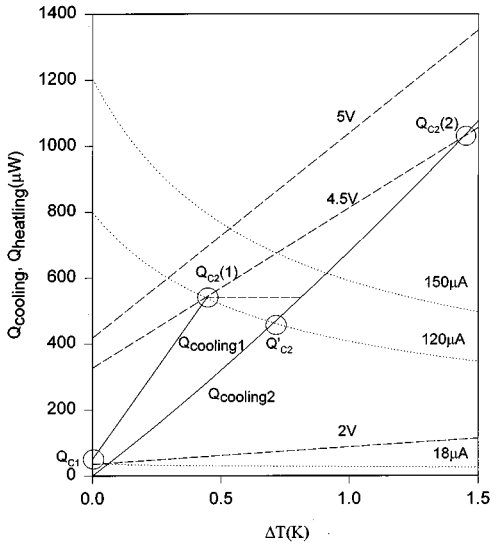

FIG. 12. Graphical solution of steady-state solutions, where $Q_{\text{heating}}=Q_{\text{cooling}}$. Solid lines: cooling powers of two different channels labeled ''cooling1'' (evaporation mechanism) and ''cooling2'' (conduction to mounting block). Dotted lines are heating powers in the constant-current mode, and dashed lines are heating power in the constant-voltage mode.

helium film plays the major role in carrying away the heat. When this channel provides the cooling power, ΔT can be approximately written as

$$\Delta T=\begin{cases}0 & \text{when } Q_{\text{cooling1}}<Q_{C1}\\ r_K(Q_{\text{cooling}}=Q_{C1}) & \text{when } Q_{C1}<Q_{\text{cooling1}}<Q_{C2},\end{cases} \tag{14}$$

based on the assumption that below Q_{C1}, the temperature rise ΔT is negligible and between Q_{C1} and Q_{C2}, ΔT is approximately proportional to the cooling power, with the coefficient obtained from the slope in Fig. 9. The second cooling channel is through the GE varnish to the copper block. There are several factors to be taken into account here, such as heat conduction through the surrounding helium gas, and the thermal boundary impedances in the sandwich structure of sample-varnish copper. Calculation estimates show that these are relatively unimportant in our experimental arrangement. The thermal conductivity of the varnish in the relevant temperature range 1–4 K is given by[24]

$$K_{\text{varnish}}=3\times10^{-4}T^{0.45}\ \text{W/cm K}, \tag{15}$$

which leads to a cooling power of the second channel equal to

$$Q_{\text{cooling2}}=(A/t)K_{\text{varnish}}(T)\Delta T. \tag{16}$$

A and t are, respectively, the area and thickness of the varnish layer, approximately 5 mm^2 and 0.3 mm, and T is approximated by a temperature midway between that of the sample and the ambient. By plotting the functions given in Eqs. (12)–(16), one obtains a graphical solution for the ΔT expressed in Eq. (10). This is shown in Fig. 12, where numbers comparable to the experimental situations for curve 1 in Fig. 5 are used. In Fig. 12, calculated heating powers versus ΔT are shown by the dotted lines for three currents, 18, 120, and 150 μA. Similar curves are shown by the dashed lines for constant voltages of 2, 4.5, and 5.0 V. One sees that for $Q_h<Q_{C1}$ (e.g., $V=2$ V line or $I=18$ μA line), the graphical solutions give $\Delta T=0$ as expected. When a current or voltage whose heating power Q_h exceeds Q_{C1} is reached, ΔT starts to increase along with Q_h until $Q_{C2}(1)$ is reached. In this region the curves for the voltage-controlled and the current-controlled modes are equivalent. At $Q_{C2}(1)$, the cooling line Q_{cooling1} stops, forcing the voltage-controlled heating line, Q^V_{heating}, to jump to the second cooling line. The interception point of Q^V_{heating} and Q_{cooling2}, $Q_{C2}(2)$, determines the sample temperature after the jump. The heating power at the interception shown in Fig. 12 is about 1 mW, which is in reasonable agreement with the experimental value, 1.1 mW. (This *quantitative* agreement should not be taken too seriously, since the estimate of K_{varnish} could easily vary by a factor of 2 from the value we extrapolated to temperatures below 3 K, using Ref. 24.) Thus, the instability in the voltage-controlled I-V curves is simply a manifestation of this switch from one to another cooling mechanism. On the other hand, the discontinuity of the first cooling line at Q_{C2} cannot force the current-controlled heating line to jump to Q'_{C2}, because $Q'_{C2}<Q_{C2}$, and a switch to the second cooling channel is not self-sustainable. Therefore, it remains at Q_{C2}. When the current continues to increase after that point, the heating line Q^I_{heating} should follow a constant-power line, as shown in the graph by a horizontal line. An immediate consequence of this is that the voltage decreases from its value V_{C2}. This is the explanation of the negative differential conductivity (dI/dV) region in Fig. 11. This process continues until the second cooling line is met, after which the two heating curves again become identical. An experiment was actually carried out in bulk liquid helium for the temperature dependence of the current at higher voltage than V_{C2}. In this condition, the temperature of the sample is the same as that of the bulk helium, and by comparing the current in the bulk liquid-helium condition to that in the film condition at the same voltage, the temperature of the sample in the latter condition after the jump can be retrieved. The results are within about 10% of the estimate based on Eq. (12).

We now examine the possibility of an intrinsic mechanism for the instability, which was mentioned in the introduction. In fact, there is indeed a singularity in our formalism which is shown by substituting Eq. (12) into Eq. (9), and utilizing Eq. (14b):

$$I=[f_2(V)(c_1+c_2T_0)-c_2f_2(V)R_kQ_{C1}]/[1-c_2f_2(V)R_kV]. \tag{17}$$

The singularity occurs at

$$c_2f_2(V)VR_k=1, \tag{18}$$

which is also the point where $dI/dV=\infty$. However the solutions of Eq. (18) by using the R_k obtained in Fig. 9 are consistently larger than the actual values by about 2 V. In addition, Eq. (18) cannot describe the observed S-shaped $I-V$ curves. Thus, the intrinsic mechanism cannot account for our experiments.

E. Other properties

We have described the principal experimental measurements which lead to the model that we constructed. Additional consequences of these types of instabilities have been reported in the literature on other systems, in particular transient or delayed phenomena, in which the time for the sample temperature to reach steady state after turning on the power can range from a few seconds to a few hundred seconds. A ''step effect'' [13] has also been reported in which a transient effect is observed in two steps, rather than as a gradual process. Effects resembling these have been observed in our experiments as well. We have also observed magnetic-field-induced jumps, which almost certainly are associated with altered heat rates resulting from the large magnetoresistance. Discussion of these phenomena will be taken up in a future publication.

V. CONCLUSIONS

An instability associated with the *S*-shaped *I*-*V* characteristic in the persistent photoconductivity of CdS has been observed. The heat transport between the interface of CdS and film-He-II, in combination with the temperature dependence of the PPC on temperature, is claimed to be responsible for the instability. Two related effects, anomalous power dependence of the Kapitza resistance and peak heat flux have been studied for our experimental configuration. The sample used in this work is particularly advantageous since by varying the light dose it can probe a very wide range of heating power without changing the electrical field. Also this work provides a reference on the heat transport problem in a configuration which is simple and practically useful in the studies of electrical and optical properties of solid in the helium temperature region.

*Present address: Physics Department, Drew University, Madison, New Jersey 07940.

[1] H. X. Jiang, D. Baum, and A. Honig, J. Lumin. **40&41**, 557 (1988).
[2] D. Baum, H. X. Jiang, and A. Honig, J. Lumin. **40&41**, 119 (1988).
[3] M. Reed and A. Honig (unpublished).
[4] See M. Reed, Ph.D thesis, Syracuse University, 1983.
[5] M. Dong and A. Honig, Bull. Am. Phys. Soc. **39**, 790 (1994).
[6] D. Baum, J. Y. Lin, and A. Honig, Bull. Am. Phys. Soc. **33**, 301 (1988).
[7] For a review of early work on this subject, see A. F. Volkov and Sh. M. Kogan, Usp. Fiz. Nauk. **96**, 633 (1968) [Sov. Phys. Usp. **11**, 881 (1969)].
[8] Ch. Karakotsou, J. A. Kalomiros, M. P. Hanias, A. N. Anagnostopoulos, and J. Spyridelis, Phys. Rev. B **45**, 11 627 (1992).
[9] B. I. Shklovskii, M. S. Shur, and A. L. Efros, Fiz. Tekh. Poluprovodn. **xx**, xxx (19xx) [Sov. Phys. Semicond. **5**, 1682 (1972)].
[10] J. D. N. Cheeke, B. Hebral, J. Richard, and R. R. Turkington, Phys. Rev. Lett. **32**, 658 (1974).
[11] B. W. Clement and T. H. K. Frederking, Pure Appl. Cryogenics **6**, 49 (1966).
[12] For a general review, see E. T. Swartz and R. O. Pohl, Rev. Mod. Phys. **61**, 605 (1989).
[13] J. C. Bishop and J. C. A. van der Sluijs, J. Low Temp. Phys. **39**, 93 (1980).
[14] D. White, O. D. Gonzales, and H. L. Johnston, Phys. Rev. **89**, 593 (1953).
[15] R. B. Duncan, G. Ahlers, and V. Steinberg, Phys. Rev. Lett. **38**, 58 (1987).
[16] M. Dingus, F. Zhong, and H. Meyer, J. Low Temp Phys. **65**, 185 (1986).
[17] D. Frank and V. Dohm, Phys. Rev. Lett. **62**, 1864 (1989).
[18] *Properties of Liquid and Solid Helium*, edited by J. Wilks (Clarendon, Oxford, 1967), p. 413.
[19] M. K. Sheinkman and A. Ya. Shik, Fiz. Tekh. Poluprovodn. **10**, 209 (1976) [Sov. Phys. Semicond. **10**, 128 (1976)].
[20] J. C. Mester, E. S. Meyer, M. W. Reynolds, T. E. Huber, and I. F. Silvera, Phys. Rev. Lett. **68**, 3068 (1992).
[21] D. Goodstein and M. Weimer, Surf. Sci. **125**, 227 (1983).
[22] E. T. Swartz and R. O. Pohl, Appl. Phys. Lett. **51**, 2200 (1987).
[23] G. L. Pollack, Rev. Mod. Phys. **41**, 48 (1969).
[24] J. H. McTaggart and G. A. Slack, Cryogenics **9**, 384 (1969).